A Neural-Network Based Real-Time SISO Controller: Real-Time Convergent Feedback Loop (RTCFL)

Mihir Savadi
Bradley Department of Electrical and Computer Engineering
Virginia Tech
May 4, 2022
mihirsavadi1@vt.edu

Abstract

PID control feedback loops are truly ubiquitous amongst a wide variety of controls and automation processes in the modern world. However, before being released, in order to achieve adequate performance, they require manual tuning by a human with domain specific knowledge. This paper proposes the Real-Time Convergent Feedback Loop (RTCFL) – a generally applicable approach that converges upon good control performance of any system over time without human input, whilst being risk-averse enough to be trained online and in real-time. In addition, the 'Control-Feedback Testbench' (CFT) – a software environment for simulation of control-feedback loops – is showcased.

Contents

1. Introduction

PID (potential, integral, derivative) control loops are ubiquitous in our world today – it is the de-facto control mechanism behind ovens, toasters, home or auto HVACs, cruise controls, auto pilots, attitude control in drones, and various industrial processes. Its popularity is due to its simplicity, reliability, and interpretability – it has been commonplace in industry for several decades. One drawback of the PID control mechanism is that the parameters that govern them require manual human tuning via trial and error. In many applications this may be inconvenient or costly. This paper proposes an approach that, for any system (or plant) thrown under its purview, can automatically converge upon equivalent behavior of an ideally tuned PID control loop (i.e. achieve perfect damping[1]), given real-time data fed to it from the system/plant it is controlling, and no human input. The architecture of this approach will be referred to as the Real-Time Convergent Feedback Loop (RTCFL).

For those unfamiliar, the basics of PID controller's will be outlined – they are remarkably simple. Motivations for this project will then be explained, before covering the architecture of the software testbench that was built in order to efficiently and scalably facilitate the simulation and testing of any arbitrary controller-plant circuit. Finally, the architecture of the RTCFL will be discussed and its performance evaluated.

2. PID Controllers Explained

Say we had an oven that we wanted to control the temperature of. The intended temperature can be set to any value in a given range by a cook, and the actual temperature of the oven would then be influenced by a heating coil within it. This heating coil would be controlled by some electrical circuitry (often times mechanical![2]) that would carefully alter the power of the heating coil such that a steady temperature is maintained. If the oven is already at a steady temperature, and the cook increases the intended temperature, the controller would then be responsible for ramping up power of the coil so that the oven is able to settle at the new temperature quickly, but not overshoot or oscillate around it (i.e. it must ensure a *perfectly damped*[1]

[1] https://en.wikipedia.org/wiki/Damping

[2] Bimetallic strips are commonly found controlling car blinkers – making sure their switching frequency is constant; or the temperature control in mini-fridges.

response). The inverse of the same logic applies if the cook decreased the temperature instead.

In this example, our oven is our system that we are concerned about, which we will refer to as the **plant**. The output characteristic of our plant that we wish to control is the temperature, which varies with time – we will refer to it as $y(t)$. The input to our plant that our controller control's in order to influence $y(t)$ is the power of the heating coil, which also varies with time – we will refer to it as $u(t)$. The intended value of $y(t)$ – as decided by any agent, in our example the cook sets an intended temperature – can also vary with time and will be referred to as $r(t)$. The error between the intended and the actual plant output will be referred to as $e(t)$. Eq 1 defines a PID controller.

$$u(t) = K_P e(t) + K_I \int_0^t e(\tau)\,\mathrm{d}\tau + K_D \frac{\mathrm{d}e(t)}{\mathrm{d}t} \quad (1)$$
$$\text{where } e(t) = r(t) - y(t)$$

In Section 1 we mentioned how PID controllers have parameters that require manual tuning – these are K_P (called the potential), K_I (called the integral), and K_D (called the derivative), which can be seen in Eq 1. Figure 1 is a block diagram representation of Eq 1, which should help illustrate the real-time nature of this type of system. It can be observed that PID controllers are Single-Input Single-Output systems (SISO).

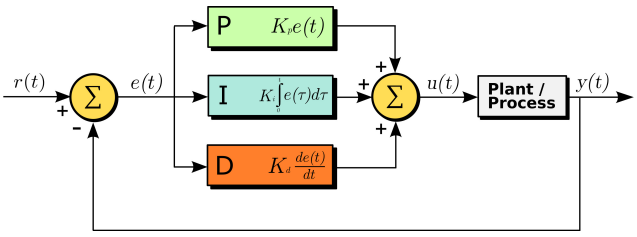

Figure 1. Block diagram of a PID controller.[18]

Considering that we will be operating in discrete time due to the digital nature of our computational platforms, Eq 2 below is the 'digital' version of Eq 1.

$$u[t] = K_P e[t] + K_I \sum_{i=0}^{n} e[t-i] + K_D\left(e[t] - e[t-1]\right)$$
$$\text{where } e[t] = r[t] - y[t], \text{and } n \geq 0 \quad (2)$$

3. Motivation

In certain situations, relying on PID control systems to achieve control stability is impractical. A common example would be when one-off systems, that aren't massed produced and don't have R&D time before mass production, need to be tuned. For example, whenever an amateur racing drone pilot builds a new custom drone with an off-the-shelf flight controller, they then assume the burden of tuning the PID parameters that govern their drone's flight characteristics. This involves flying around, observing flight behavior, and tuning iteratively via trial-and-error – this is clearly cumbersome and can even lead to situations that may damage this one-off drone. Modern flight control software comes with auto-tuning features, but these are mostly deterministic and perform poorly.

Another example would be DIY reflow ovens. When hobbyists or independent printed circuit board designers want to build large complex boards or boards with several hard-to-hand-solder surface mount devices, they often seek the refuge of 'reflow-ovens'. The reflow oven process involves a PCB with components placed onto their footprints with unsoldered 'solder paste' in between. This PCB is then placed into a reflow oven, which controls the temperature in its chamber to follow a very specific temperature-time curve in order for the solder paste to melt and create sound solder joints as per the manufacturers specifications. Often times hobbyists modify toaster ovens into reflow ovens (which are very popular and work remarkably well) by swapping out existing cheap mechanical controls with their own programmed PID controllers, which they then have to tune. If instead they could use an auto-tuning 'adaptive' controller, it would make the conversion process of any randomly chosen toaster oven a lot easier.

Similar arguments from the examples above can be used to justify the benefits of such an 'adaptive' controller in various industrial applications. As such, many efforts have already been made and are currently even being used in deep industry (see references), however many remain seemingly proprietary. The RTCFL approach (detailed in Section 5) is not one that has been explicitly observed yet in existing literature.

4. Control-Feedback Testbench Architecture

In order to efficiently build, analyze, and maintain a variety of control-feedback circuit designs without compromising design flexibility and granularity, the use of a modular 'testbench' environment/platform was imperative. Such a testbench, simply referred to as the 'Control-Feedback Testbench' (or CFT), was built as such to facilitate the exploration of the RTCFL proposed in this paper. Hopefully, by the end of this section the reader will recognize it's utility beyond just the scope of this paper.

The testbench implemented is fundamentally modular, employing object orientated design with heavy use of both inheritance (to enforce inter-class communication consistency without compromising modularity) and composition. At its core, the testbench is based on the 'actor' paradigm, whereby each element in any given circuit (e.g. in Figure 1

or 3 for example) is treated as a black box, or an actor, whose basic inputs and outputs are standardized by an abstract actor base class, and whose internal calculations are abstracted away. Actors can be controllers, plants, or any other influencing element of a circuit.

Actor objects are then instantiated inside a circuit class, which contain standardized inputs and outputs themselves, and abstract away the interconnections (whether chronological or parallel) between whatever actors may be present in said particular circuit. These standardizations are again enforced by an abstract circuit base class. Circuit classes contain a single function to update actor outputs according to its defined interconnections for each time-step, as well as store historical data for each 'wire' in the circuit.

Finally, a scheduler class is what the user interacts with in order to utilize the testbench – it contains an instance of a particular circuit class, whose parameters are determined on initialization of a scheduler object; it provides a function to get inputs into the circuit, either by time-step by time-step polling or by parsing an external text file; it provides a function to probe the circuit to get information on its stored current and historical data; and it provides a function to generate a convenient plot to quickly visualize circuit behavior, e.g. Figure 2, ??, ??, ??.

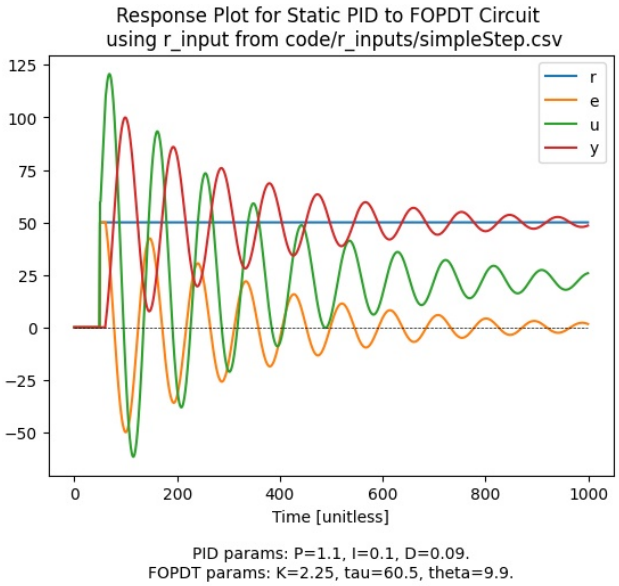

Figure 2. Example output plot generated by the CFT for a simple PID controller + FOPDT plant, where the PID controller is not well tuned – the control-feedback loop is under damped. Refer to fig 1 for plot label references.

The user can create arbitrary actor classes (controllers, plants, etc.) and circuit classes, which will function predictably with the aforementioned scheduler class, as long as the respective abstract base classes are adhered to. Thus, a user can use the scheduler class of this testbench to automate testing and analysis of a variety of controllers, plants, and circuits, in an arbitrarily simulated real-time environment.

5. The RTCFL Approach

In order to understand the RTCFL approach, the interconnects between each actor in the circuit shown in Figure 3 must first be studied. As is almost immediately obvious, the RTCFL is model-based. Section 5.1 walks through the RTCFL approach step-by-step, and Section 5.2 evaluates its performance.

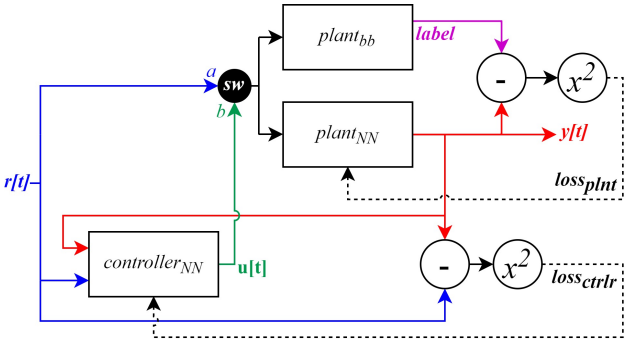

Figure 3. RTCFL circuit diagram. Each square box represents an actor: $plant_{bb}$ is the original black-box plant that $plant_{NN}$ seeks to emulate; $controller_{NN}$ is the NN that ultimately needs to be trained to achieve optimal plant control. Each actor can either be 'dormant' or 'active' from the point of view of the circuit. The NN based actors handle and switch between 'learning' and 'inference' modes within themselves. The black circle labelled 'SW' acts as a switch redirecting either the $r[t]$ vector on its a channel or the $u[t]$ vector on its b channel into both the plants. The $r[t]$, $u[t]$, $y[t]$ vectors follow the convention shown in Fig 1. The black dotted vectors indicate objective function output values used to train their respective NN's via gradient descent.

5.1. High Level Architecture

Refer to the description of Figure 3 for a basic explanation of the function of each element in the circuit shown. The steps below will outline the series of operations within the circuit that defines the RTCFL approach. Note that $plant_{NN}$ exists to enable training of $controller_{NN}$ in later steps of the RTCFL approach via backpropagation, by providing a known function through which the derivative of the loss function with respect to the parameters of $controller_{NN}$ can be calculated – this would not be possible with the 'black box' that is $plant_{bb}$, where it's inner function is unknown.

Just for the sake of simulation testing $plant_{bb}$ is initialized as an arbitrary FOPDT (first order plus dead time) model. The RTCFL circuit was tested with $plant_{NN}$ and $controller_{NN}$ being implemented as DNN's in one instance (with inputs being a fixed vector of up to [t-n] time

series data), and RNN's in another. Their architectures can as such be experimented with without altering overall RTCFL approach – the CFT enables this flexibility.

Step 1

SW is set to pass its a signal and block its b signal. $controller_{NN}$ is disabled, $plant_{bb}$ and $plant_{NN}$ (initialized with random weights) are enabled.

$r[t]$ signals are chosen with enough temporal variation to encapsulate what is typical of whatever the chosen application space is. These are then passed concurrently into both plants, whereby $plant_{bb}$'s output is treated as a label, against which $plant_{NN}$'s output is used to calculate a loss value – $loss_{plnt}$.

As time goes on, an internal data base is appended to with $r[t]$ time series data (with a variable 'n' number of time-steps into the past), along with associated $y[t]$ and $label$ (that is $plant_{bb}$'s output) data. The interval with which this happens is flexible. Then, at another variable-number of time steps, this data base is used to aggregate $loss_{plnt}$, which is then backpropagated through $controller_{NN}$, after which $controller_{NN}$'s parameters are updated and the database is reset to empty. This is repeated until $loss_{plnt}$ reaches a minimum threshold value, $minloss_{plnt}$ (left as a variable), after which we can move on to step 2.

Step 2

SW now blocks its a signal and passes its b signal. $plant_{bb}$ is disabled, $plant_{NN}$ and $controller_{NN}$ are enabled.

Ideally, $controller_{NN}$ is initiated with pre-trained weights such that it emulates a safe/generally applicable but poorly performing PID controller – this allows the benefit of being able to train and optimize $controller_{NN}$'s weights online and in real-time without risk of throwing the plant out of its safety margins (which would be the case initially with random weights). The possibility of this allows for a room to avert plant-hazard risks in real-life applications.

The objective function described in Eq 3 represents, in more detail, the loss function represented by $loss_{ctrlr}$ in Figure 3. From Figure 1 we know that $e[t] = r[t] - y[t]$, so $loss_{ctrlr}$ penalizes for either under or over damping, and is the lowest at perfect damping. It can be seen that the $loss_{ctrlr}$ function is just a regular mean squared error, which is a convenience the RTCFL can enjoy.

$$loss_{ctrlr} = \frac{1}{z+1}\sum_{i=0}^{z}\left(r[t-i] - y[t-i]\right)^2 \quad \text{where } z \geq n \tag{3}$$

A similar approach to the training of $plant_{NN}$ in step 1 is executed here in step 2 to train $controller_{NN}$. This time $r[t]$ and $y[t]$ time series data (of a variable 'n' number of time-steps into the past) is appended into a database, along with associated loss value. The interval with which this happens is flexible, as well as the interval at which backpropagation, $controller_{NN}$ parameter update, and database reset happens.

Step 3 (optional)

The benefits of the RTCFL can be especially be exploited if we consider that $plant_{NN}$ can be continually optimized in parallel to the operation of $controller_{NN}$, which can also continually undergo training in parallel to inference through a proxy network. This would be valuable in environments that may change with time such that the fundamental dynamics of a plant may change with it too, e.g. an aircraft passing through different atmospheric layers and perhaps into space even, where fluctuations in air pressure, temperature, and even weather may significantly alter flight dynamics in unpredictable non-linear ways. In a nutshell, the multi-path nature and repeated computational 'blocks' of the RTCFL circuit allows significant room for parallel computation, dynamic network training, and even hardware acceleration at the RTCFL system level (i.e. furthering potential power-performance-area optimizations in FPGA or custom silicon implementations), which can be exploited depending on the application.

5.2. Testing Results, Evaluations, and Conclusions

Two implementations of the RTCFL were created with Pytorch – one where the NN actors we're based on DNN's, and another based on RNN's. Different actor classes, circuit classes and test programs utilizing the CFT were built. (TODO FOOTNOTE TO GITHUB HERE FOR EACH) Said classes were built with a high-degree of flexibility in NN architecture and training configuration, which allowed for flexible experimentation. Both implementations used the AdamW optimizer for gradient descent.

It should be noted that due to the real-time nature of the RTCFL, typical training, test, and validation sets are not applicable. Rather, different sequences of $r[t]$ values are used to feed into the circuit in 'simulated real-time' via the CFT (LINK TO GITHUB HERE).

The main experiment used a 10-million long random sequence of $r[t]$ values were generated with a script (TODO GITHUB LINK HERE TO SCRIPT and input sequence) that allowed for configuration in step-size and step-width. These inputs were then fed into the aforementioned RNN and DNN RTCFL architectures, along with a vanilla static PID circuit (like in Figure 1) for reference. Figures 4, 5, and 6 show the plots of these experiments, as generated by the CFT, for the RTCFL-DNN, RTCFL-RNN, and static PID circuits respectively.

As can be seen, in both the DNN and RNN RTCFL cases, the error (e) plots and the $controller_{NN}$ and $plant_{NN}$ plots (labelled u and y respectively) were extremely poor. Often times NN outputs would be close to zero, implying the existence of vanished gradients. These problems were mostly

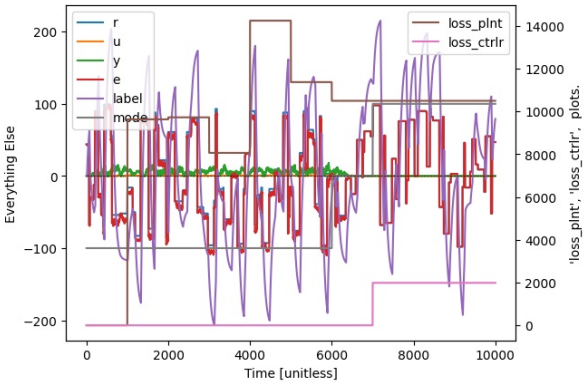

DNN based RTCFL Parameters are:
Plant_bb : <control_feedback_testbench.plants.FOPDT object at 0x00000287C7B41C10>
Plant_NN model : NN(
  (_layerList): ModuleList(
    (0): Linear(in_features=500, out_features=750, bias=True)
    (1): ReLU()
    (2): Linear(in_features=750, out_features=750, bias=True)
    (3): ReLU()
    (4): Linear(in_features=750, out_features=1, bias=True)
    (5): ReLU()
)
)
Plant MinLoss : 5
Plant k : 1
Plant l : 1000
Plant_bb model : <control_feedback_testbench.plants.FOPDT object at 0x00000287C7B41C10>
Controller_NN model : NN(
  (_layerList): ModuleList(
    (0): Linear(in_features=1000, out_features=750, bias=True)
    (1): ReLU()
    (2): Linear(in_features=750, out_features=750, bias=True)
    (3): ReLU()
    (4): Linear(in_features=750, out_features=1, bias=True)
    (5): ReLU()
)
)
Controller MinLoss : 2000
Controller k : 1
Controller l : 1000

Figure 4. RTCFL-DNN circuit experiment result.

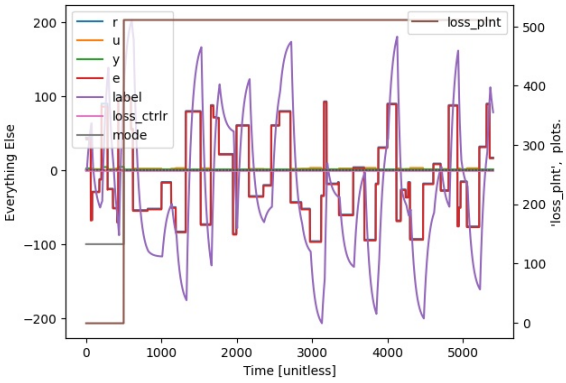

RNN based RTCFL Parameters are:
plant_bb_model : <control_feedback_testbench.plants.FOPDT object at 0x0000020E086BBAC0>
plant_NN_model : RNN(
  (_LinearLayer): Linear(in_features=2, out_features=1, bias=True)
  (_ReLULayer): ReLU()
)
controller_NN_model : RNN(
  (_FirstLinearLayer): Linear(in_features=3, out_features=1, bias=True)
  (_LinearLayer): Linear(in_features=2, out_features=1, bias=True)
  (_ReLULayer): ReLU()
)
plant_nn_trainSeqLen : 5
plant_nn_trainSeqAddPeriod : 5
plant_nn_trainSeqDBSize : 100
plant_nn_minLoss : 150000
controller_nn_trainSeqLen : 50
controller_nn_trainSeqAddPeriod : 50
controller_nn_trainSeqDBSize : 100
controller_nn_minLoss : 3

Figure 5. RTCFL-RNN circuit experiment result.

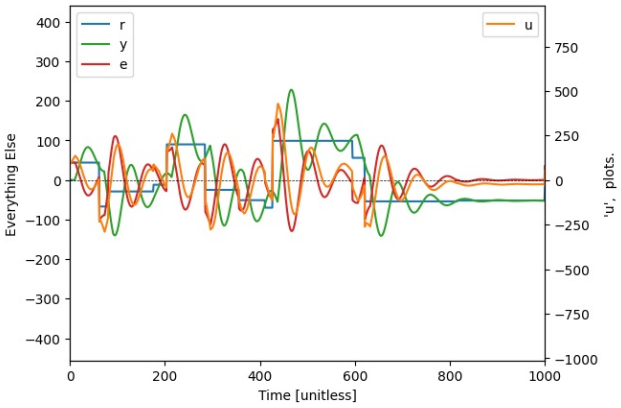

PID params: P=2, I=0.1, D=0.2.
FOPDT params: K=2.25, tau=60.5, theta=9.9.

Figure 6. Static PID circuit experiment result.

attributed to the time spent on dialing in the various actor variables – this aspect of 'meta-tuning' proved to be extremely challenging. Given the plausibility of the RTCFL approach, it is reasonable to project potential successful and conclusive results in the future; that is given more testing and experimentation with different actor architectures (like LSTM's or Attention and Transformer Networks).

For all the RTCFL's pros, there exists notable cons that require especially tuned networks to handle them. Firstly, the RTCFL would only be able to perform well in systems with really high sample rates, in order to collect enough data to achieve fast enough convergence. With the need for high sample rates, there is also a need for proportionally high temporal variation in input data in order to capture plant dynamics more generally. But with these high sample rates comes the need for more complex architectures and high memory requirements in order to 'remember' enough past data to produce well informed outputs. For example, an RTCFL would probably not work in controllers for slow-changing high-thermal-capacity plants like in some oversized industrial HVAC systems. Ultimately, these issues are a result of RTCFL's real-time nature and having to work with sparsely available data.

Please see github here and here and here.

References

[1] Andrew G. Barto. Reinforcement learning control. *Current Opinion in Neurobiology*, 4(6):888–893, 1994. https://www.sciencedirect.com/science/article/pii/0959438894901384.

[2] Debmalya Biswas. Reinforcement learning based hvac optimization in factories. In *Proceedings of the Eleventh ACM International Conference on Future Energy Systems*, e-Energy '20, pages 428–433, New York, NY, USA, 2020. Association for Computing Machinery. https://doi.org/10.1145/3396851.3402363.

[3] Debmalya Biswas. Data-driven (reinforcement learning-based) control, Feb 2022. https://towardsdatascience.com/data-driven-control-d516ca28047c.

[4] Silvia Ferrari and Robert F. Stengel. *An adaptive critic global controller*, volume 4, pages 2665–2670. 2002.

[5] Zhe Guan and Toru Yamamoto. Design of a reinforcement learning pid controller. In *2020 International Joint Conference on Neural Networks (IJCNN)*, pages 1–6, 2020.

[6] M.T. Hagan and H.B. Demuth. Neural networks for control. In *Proceedings of the 1999 American Control Conference (Cat. No. 99CH36251)*, volume 3, pages 1642–1656 vol.3, 1999.

[7] Martin T. Hagan, Howard B. Demuth, and Orlando De Jesús. An introduction to the use of neural networks in control systems. *International Journal of Robust and Nonlinear Control*, 12(11):959–985, 2002. https://onlinelibrary.wiley.com/doi/abs/10.1002/rnc.727.

[8] Andrej Karpathy. The unreasonable effectiveness of recurrent neural networks. *https://karpathy.github.io/2015/05/21/rnn-effectiveness/*, 2015.

[9] Ayub I. Lakhani, Myisha A. Chowdhury, and Qiugang Lu. Stability-preserving automatic tuning of pid control with reinforcement learning. 2021. https://arxiv.org/abs/2112.15187.

[10] F.W. Lewis, S. Jagannathan, and A. Yesildirak. *Neural Network Control Of Robot Manipulators And Non-Linear Systems*. CRC Press, 2020.

[11] Nicholas Lewis. Emulating a pid controller with long short-term memory, series. *towardsdatascience.com*, 2020.

[12] Derong Liu. An introduction to adaptive critic control: A paradigm based on approximate dynamic programming. 2006.

[13] W. Thomas Miller, Richard S. Sutton, and Paul J. Werbos. *Computational Schemes and Neural Network Models for Formation and Control of Multijoint Arm Trajectory*, pages 197–228. 1995.

[14] D.H. Nguyen and B. Widrow. Neural networks for self-learning control systems. *IEEE Control Systems Magazine*, 10(3):18–23, 1990.

[15] Christopher Olah. Understanding lstm networks. *https://colah.github.io/posts/2015-08-Understanding-LSTMs/*, 2015.

[16] Steven Spielberg Pon Kumar, Aditya Tulsyan, Bhushan Gopaluni, and Philip Loewen. A deep learning architecture for predictive control. *IFAC-PapersOnLine*, 51(18):512–517, 2018. 10th IFAC Symposium on Advanced Control of Chemical Processes ADCHEM 2018.

[17] Luthfi Ramadhan. Radial basis function neural network simplified, Nov 2021. https://towardsdatascience.com/radial-basis-function-neural-network-simplified-6f26e3d5e04d.

[18] Arturo Urquizo. Pid.svg, 2008. https://commons.wikimedia.org/wiki/File:PID.svg.

[19] Rebecka Winqvist. Neural network approaches for model predictive control. 2020. https://www.diva-portal.org/smash/record.jsf?pid=diva2%3A1477561&dswid=-1462.

[20] Jun Zhao, Qingliang Zeng, and Bin Guo. Adaptive critic learning-based robust control of systems with uncertain dynamics. *Computational Intelligence and Neuroscience*, 2021:1–8, 11 2021.

License